

PROCEEDINGS OF SPIE

[SPIDigitalLibrary.org/conference-proceedings-of-spie](https://spiedigitallibrary.org/conference-proceedings-of-spie)

High accuracy wavefront reconstruction with slope and coordinate compensation

Yiyu Li, Wei Huang, Siyun Chen, Jiaojie Chen, Haihua Feng, et al.

Yiyu Li, Wei Huang, Siyun Chen, Jiaojie Chen, Haihua Feng, Hao Chen, "High accuracy wavefront reconstruction with slope and coordinate compensation," Proc. SPIE 10847, Optical Precision Manufacturing, Testing, and Applications, 1084706 (12 December 2018); doi: 10.1117/12.2503942

SPIE.

Event: International Symposium on Optoelectronic Technology and Application 2018, 2018, Beijing, China

High accuracy wavefront reconstruction with slope and coordinate compensation

Yiyu Li^{*}, Wei Huang, Siyun Chen, Jiaojie Chen, Haihua Feng, Hao Chen
School of Optometry and Ophthalmology, Wenzhou Medical University, Wenzhou, Zhejiang,
325027, China

ABSTRACT

The conventional wavefront reconstruction of the Shack-Hartmann method is based on the measured slopes by using the least-square fitting method. However, this reconstruction method suffers from the low order Zernike terms in wavefront, especially defocus and astigmatism, due to the discrepancy of coordinate systems between the lenslet array and the original wavefront caused by the propagation of subaperture wavefront. In this paper, a ray tracing method was used to calculate the slope error between an input wavefront and the reconstructed wavefront. Then, an iteration procedure including slope compensation and coordination compensation was constructed and implemented to minimize the wavefront reconstruction error. The numerical simulation was performed for a variety of defocus-dominated input wavefront and high-order-dominated input wavefront, and verified that high accuracy wavefront reconstruction can be achieved by the proposed iterative compensation method.

Keywords: Wavefront; Ray tracing; Shack-Hartmann; Zernike polynomial

1. INTRODUCTION

Shack-Hartmann wavefront sensor can detect the incident wavefront (IW) by the array of lenslets and generate an array of focal spot on the digital camera. The IW can be reconstructed from the data of local wavefront slopes derived from the focal spot shift with respect to the optical axis of the respective lenslet^{1,2}. The ideal wavefront reconstruction requires both the measured wavefront slopes and the exact locations of the slopes on the original IW which however is unknown during the measurement. Therefore, the conventional reconstruction algorithms have used the coordinates of the respective lenslet center for an approximation solution^{3,4}. The propagation of subaperture wavefront from the lenslet back to the original IW is responsible for creating the discrepancies in the coordinate measurement. This coordinate error through the entire reconstruction algorithm eventually results in the error in the reconstructed wavefront especially when the second order Zernike modes dominate in the IW. As we know, the slope measurement errors caused by the noise in the slope measurement has deserved particular attention⁵⁻⁸. However, the coordinate errors which decide the preference of a specific reconstruction algorithm are seldomly investigated. To eliminate the coordinate errors, we developed an iterative compensation procedure including the slope compensation and the following coordinate compensation. In this way, the ultra-high accuracy wavefront reconstruction was achieved by numerical simulation.

2. RECONSTRUCTION PRINCIPLE

We consider an applied wavefront W_1 to be measured by Shark-Hartmann sensor as shown in Fig. 1. One of the chief rays OP, passing through the center of lenslet, represents the normal direction $N_1(u, v, \omega)$ at the starting point T_1 on wavefront W_1 . If we assume that the aperture of thin lenslet is small enough, the intersection of chief ray and detector defines the centroid position of focal spot. The wavefront slope (S_i^x, S_i^y) at point T_1 is then evaluated by the focal spot shift. Based on the data of wavefront slope and the coordinate of center point $O(x, y, z)$ of each lenslet, the conventional reconstruction algorithms is used to generate wavefront W_2 which is an approximation of wavefront W_1 .

^{*} liyiyu@wmu.edu.cn; phone 086-577-88067922

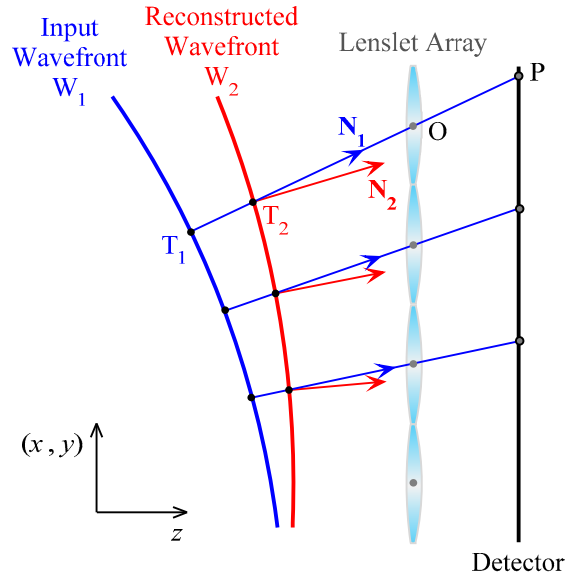


Figure 1. Wavefront detection with Shack-Hartmann sensor

In our proposed compensation method, the slope compensation is implemented first. A reverse ray tracing is calculated for the chief ray OP to find the intersection T_2 on the wavefront W_2 where the normal direction $N_2(u', v', \omega')$ can be calculated simultaneously and then compared with $N_1(u, v, \omega)$ to give the compensation of slope measurement as

$$\Delta S_i^x = -\frac{u}{\omega} + \frac{u'}{\omega'}$$

$$\Delta S_i^y = -\frac{v}{\omega} + \frac{v'}{\omega'}$$

The slope compensation $(\Delta S_i^x, \Delta S_i^y)$ are used in modal wavefront reconstruction algorithm expressed as

$$\begin{cases} S_i^x + \Delta S_i^x = \sum_{j=0}^J a_j Z_j^x(x_i, y_i) \\ S_i^y + \Delta S_i^y = \sum_{j=0}^J a_j Z_j^y(x_i, y_i) \end{cases}$$

where $i = 1, 2, \dots, n$ is the total number of grid points. The only unknown parameters in Eq. (2) are the Zernike coefficients a_j whose best estimation is the least-squares solution of the following equation:

$$\begin{bmatrix} Z^x \\ Z^y \end{bmatrix} A = \begin{bmatrix} U \\ V \end{bmatrix}$$

where

$$Z^x = \begin{bmatrix} Z_0^x(x_1, y_1) & Z_1^x(x_1, y_1) & \dots & Z_J^x(x_1, y_1) \\ Z_0^x(x_2, y_2) & Z_1^x(x_2, y_2) & \dots & Z_J^x(x_2, y_2) \\ \vdots & \vdots & \vdots & \vdots \\ Z_0^x(x_n, y_n) & Z_1^x(x_n, y_n) & \dots & Z_J^x(x_n, y_n) \end{bmatrix}$$

$$Z^y = \begin{bmatrix} Z_0^y(x_1, y_1) & Z_1^y(x_1, y_1) & \dots & Z_J^y(x_1, y_1) \\ Z_0^y(x_2, y_2) & Z_1^y(x_2, y_2) & \dots & Z_J^y(x_2, y_2) \\ \vdots & \vdots & \vdots & \vdots \\ Z_0^y(x_n, y_n) & Z_1^y(x_n, y_n) & \dots & Z_J^y(x_n, y_n) \end{bmatrix}$$

$$A = [a_0, a_1, \dots, a_J]^T$$

$$U = [S_1^x + \Delta S_1^x, S_2^x + \Delta S_2^x, \dots, S_n^x + \Delta S_n^x]^T$$

$$V = [S_1^y + \Delta S_1^y, S_2^y + \Delta S_2^y, \dots, S_n^y + \Delta S_n^y]^T$$

Thus, the newly reconstructed wavefront after slope compensation is then given by

$$W_3 = \sum_{j=0}^J a_j Z_j(x_i, y_i)$$

The remaining slope errors in wavefront W_3 will be suppressed further during the following compensation of the coordinate error.

An iteration procedure is used for the coordinate compensation. The reverse ray tracing is calculated again for the chief ray OP to find the new intersection $T_3(x', y', z')$ on wavefront W_3 and the normal direction $N_3(u', v', \omega')$ at the same point. The coordinate of T_3 which is much closer to the target T_1 as compared with the point T_2 is used to replace the original coordinate of point O in the modal wavefront reconstruction algorithm which employs the measured original wavefront slopes:

$$\begin{cases} S_i^x = \sum_{j=0}^J b_j Z_j^x(x'_i, y'_i) \\ S_i^y = \sum_{j=0}^J b_j Z_j^y(x'_i, y'_i) \end{cases}$$

where the Zernike coefficients b_j is the least-squares solution of the following equation:

$$\begin{bmatrix} R^x \\ R^y \end{bmatrix} B = \begin{bmatrix} X \\ Y \end{bmatrix}$$

$$\begin{aligned}
\mathbf{R}^x &= \begin{bmatrix} Z_0^x(x'_1, y'_1) & Z_1^x(x'_1, y'_1) & \dots & Z_J^x(x'_1, y'_1) \\ Z_0^x(x'_2, y'_2) & Z_1^x(x'_2, y'_2) & \dots & Z_J^x(x'_2, y'_2) \\ \vdots & \vdots & \vdots & \vdots \\ Z_0^x(x'_n, y'_n) & Z_1^x(x'_n, y'_n) & \dots & Z_J^x(x'_n, y'_n) \end{bmatrix} \\
\mathbf{R}^y &= \begin{bmatrix} Z_0^y(x'_1, y'_1) & Z_1^y(x'_1, y'_1) & \dots & Z_J^y(x'_1, y'_1) \\ Z_0^y(x'_2, y'_2) & Z_1^y(x'_2, y'_2) & \dots & Z_J^y(x'_2, y'_2) \\ \vdots & \vdots & \vdots & \vdots \\ Z_0^y(x'_n, y'_n) & Z_1^y(x'_n, y'_n) & \dots & Z_J^y(x'_n, y'_n) \end{bmatrix} \\
\mathbf{B} &= [b_0, b_1, \dots, b_J]^T \\
\mathbf{X} &= [S_1^x, S_2^x, \dots, S_n^x]^T \\
\mathbf{Y} &= [S_1^y, S_2^y, \dots, S_n^y]^T
\end{aligned}$$

Thus, the reconstructed wavefront after coordinate compensation is given by

$$W_4 = \sum_{j=0}^J b_j Z_j(x_i, y_i)$$

The accuracy of wavefront reconstruction can be evaluated by using the RMS normal direction errors as

$$\text{RMSNDE} = \sqrt{\frac{\sum_{i=1}^n [N_1(u, v, \omega) - N_4(u', v', \omega')]_i^2}{n}}$$

where $N_4(u', v', \omega')$ is the normal of wavefront W_4 and can be calculated by using the ray tracing method. This coordinate compensation method is repeated until the reconstructed wavefront converge. After this iteration compensation procedure, an ultra-high accuracy can be achieved for wavefront reconstruction.

3. SIMULATION RESULTS

An input wavefront (IW) containing a single Zernike mode Z_4 (or defocus) with coefficient of $c_4 = -3 \mu\text{m}$ within an aperture of 6 mm in diameter was first considered to be detected by the wavefront sensor. The IW was discretized with grid pitch of 0.06 mm to find the position of T_1 as well as the normal direction N_1 on the wavefront. According to the normal direction N_1 , the coordinate of lenslet center point O and the vector T_1O can be easily calculated as the IW intersects the plane of lenslet array at the aperture center. The conventional algorithm using the coordination of point O and the slope derived from N_1 were used to reconstruct the wavefront W_2 which was compared with the original IW to give the reconstruction error as shown in Fig 2(b). Here, Zernike polynomials up to order of $n = 16$ were employed in the modal fitting method.

The accuracy was improved with slope compensation and the following coordination compensation as shown in Fig 2(c) and Fig 2(d), respectively. Since the IW was pre-determined here, the accuracy of wavefront reconstruction can also be evaluated by the RMS wavefront reconstruction error (RMSWRE) as

$$\text{RMSWRE} = \sqrt{\sum_{j=3}^J (b_j - c_j)^2}$$

where b_j and c_j are the Zernike coefficients of the final reconstructed wavefront and the IW, respectively.

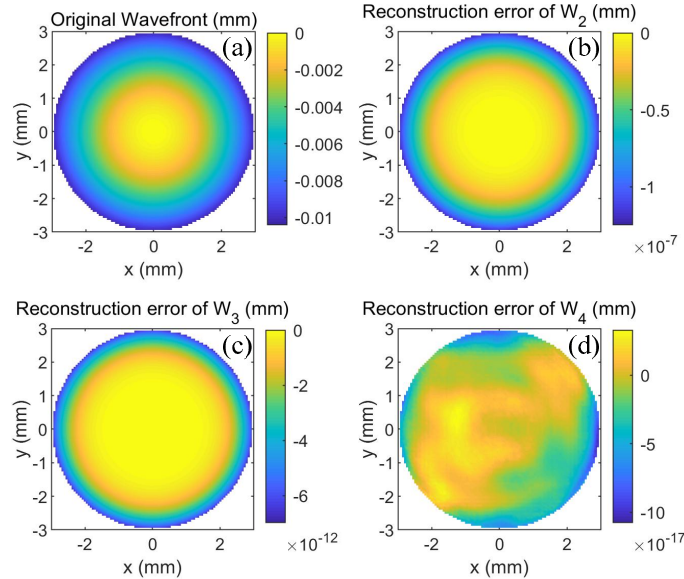


Figure 2. Reconstruction of IW composed of defocus. (a) Phase profile of the original input wavefront with $c_4 = -3 \mu\text{m}$; Reconstructed error by using (b) conventional method; (c) slope compensation method; (d) slope and coordinate compensation method.

The higher weight of defocus in IW, the more iterations of compensation will be needed for the required high accuracy wavefront reconstruction. As shown in Fig. 3, one loop of slope compensation and one loop of coordinate compensation is sufficient for the IW with $c_4 = -3 \mu\text{m}$. In the case of IW with $c_4 \leq -10 \mu\text{m}$, more loops of coordinate compensation should be implemented for the same accuracy.

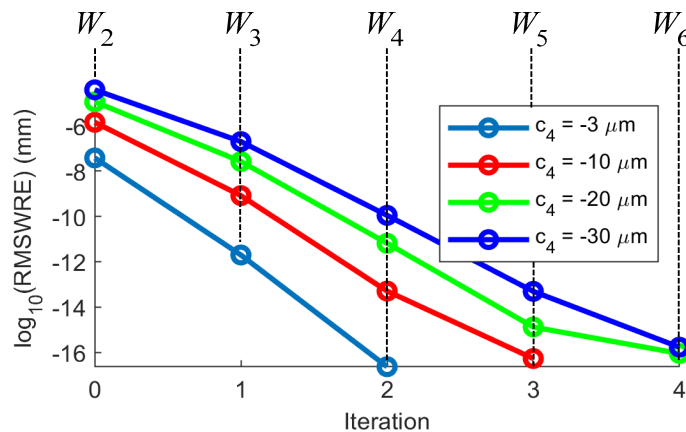


Figure 3. Iteration process and the associated RMS wavefront reconstruction error when the IW is composed of different weight of defocus.

The proposed compensation method can also be applied to the reconstruction of freeform wavefront containing only high order components that is common in adaptive optics. Fig. 4 shows such an example in which the first and the second order of Zernike terms were set to be zero in IW, while the values of the remaining high order terms were from the measured data in lab. The conventional reconstruction algorithm has performed well as shown in Fig. 4(b) due to the small variance and the limited local propagation of IW. Ultra-high accuracy of wavefront reconstruction was obtained by following the compensation method.

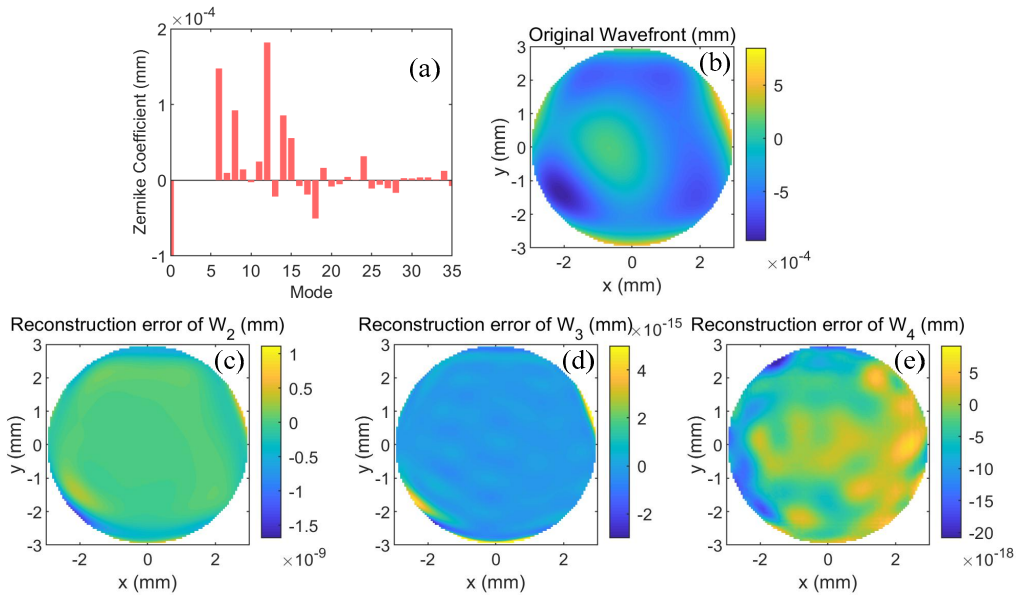


Figure 4. Reconstruction of IW composed of high order Zernike terms. (a) Values of Zernike coefficients of IW; (b) phase profile of IW; Reconstructed error by using (c) conventional method, (d) slope compensation method, (e) slope and coordinate compensation method.

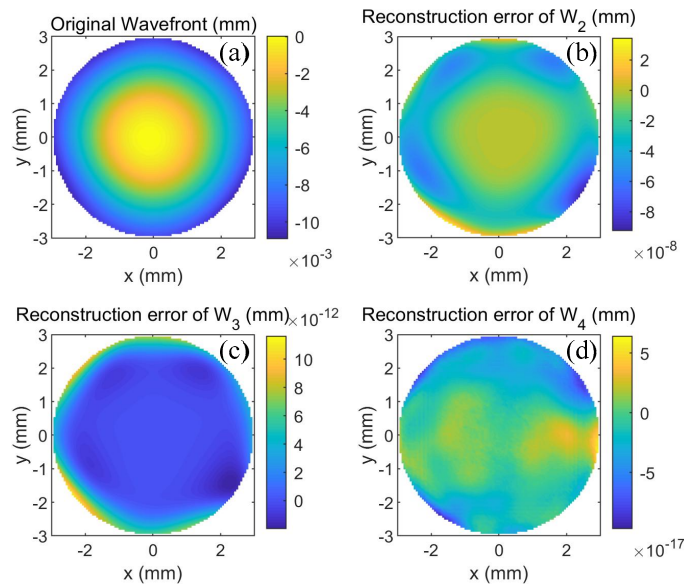


Figure 5. Reconstruction of IW composed of defocus ($c_4 = -3 \mu\text{m}$) and high order Zernike terms depicted in Fig.4. (a) Phase profile of the original input wavefront; Reconstructed error by using (b) conventional method; (c) slope compensation method; (d) slope and coordinate compensation method.

The IW shown in Fig.5(a) was the combination of the original IW from Fig. 3(a) and Fig. 4(a), such that both low order and high order Zernike term was considered in the simulation, which is common in ocular wavefront. Although the complexity of wavefront had been increased, two iterations was sufficient to obtain the accurate reconstructed wavefront with negligible errors (see Fig. 5(d)). The iteration procedure applied here was similar to that used in Fig. 2 due to the defocus-dominated IW. If we increase the weight of defocus by setting $-30 \mu\text{m} \leq c_4 \leq -10 \mu\text{m}$, ultra-high accuracy can be expected within four iterations according to the relation between RMSWRE and iteration process depicted in Fig. 3.

4. CONCLUSION

The iterative compensation procedure concerning both wavefront slope and coordinate for wavefront reconstruction was proposed and analyzed in detail. The comparison between the iterative compensation method and the conventional reconstruction method was performed over various IWs, from the simple IW containing only defocus to a highly complex IW composed of multiple Zernike modes. The numerical simulation demonstrated that the ultra-high accuracy wavefront reconstruction can be achieved by our new method.

ACKNOWLEDGMENT

The authors want to thank Junzhong Liang for valuable discussion. This research was supported by National Natural Science Foundation of China (61775171); Natural Science Foundation of Zhejiang Province (LY16H120007); Public Interest Science and Technology Program of Wenzhou (G20160033, Y20160438); National Key Research and Development Program of China (2016YFC0100200).

REFERENCES

- [1] W. H. Southwell, "Wave-front estimation from wave-front slope measurements," J. Opt. Soc. Am. 70, 998–1006 (1980).
- [2] D. M. Topa, "Wavefront reconstruction for the Shack-Hartmann wavefront sensor," Proc. SPIE 4769, 101–115 (2002).
- [3] M.C. Roggemann, T.J. Schulz, "Algorithm to increase the largest aberration that can be reconstructed from Hartmann sensor measurements," Appl. Opt. 37, 4321–4329 (1998)
- [4] M.C. Roggemann, T.J. Schulz, C. W. Ngai, and J. T. Kraft, "Joint processing of Hartmann sensor and conventional image measurements to estimate large aberrations: theory and experimental results," Appl. Opt. 38, 2249–2255 (1999)
- [5] W. Zou and J. P. Rolland, "Quantifications of error propagation in slope-based wavefront estimations," J. Opt. Soc. Am. A 23, 2629–2638 (2006).
- [6] W. Zou and Z. Zhang, "Generalized wave-front reconstruction algorithm applied in a Shack-Hartmann test," Appl. Opt. 39, 250–268 (2000).
- [7] G. Li, Y. Li, K. Liu, X. Ma, and H. Wang, "Improving wavefront reconstruction accuracy by using integration equations with higher order truncation errors in the Southwell geometry," J. Opt. Soc. Am. A 30, 1448–1459 (2013).
- [8] B. Pathak and B. R. Boruah, "Improvement in error propagation in the Shack–Hartmann-type zonal wavefront sensors," J. Opt. Soc. Am. A 34, 2194–2202 (2017)